

ORNL/CSD/TM--222

DE86 004639

ORNL/CSD/TM-222

TMI-2 CRITICALITY STUDIES: LOWER-VESSEL

RUBBLE AND ANALYTICAL BENCHMARKING

R. M. Westfall, J. R. Knight, P. B. Fox, O. W. Hermann, J. C. Turner

Date Published - December 1985

Nuclear Engineering Applications Department
Technical Applications
Computing and Telecommunications Division
Oak Ridge National Laboratory

Prepared for
The U. S. Department of Energy,
Office of Terminal Waste and
Remedial Action

This report was prepared as an account of work sponsored by an agency of the United States Government. Neither the United States Government nor any agency thereof, nor any of their employees, makes any warranty, express or implied, or assumes any legal liability or responsibility for the accuracy, completeness, or usefulness of any information, apparatus, product, or process disclosed, or represents that its use would not infringe privately owned rights. Reference herein to any specific commercial product, process, or service by trade name, trademark, manufacturer, or otherwise does not necessarily constitute or imply its endorsement, recommendation, or favoring by the United States Government or any agency thereof. The views and opinions of authors expressed herein do not necessarily state or reflect those of the United States Government or any agency thereof.

DISCLAIMER

Martin Marietta Energy Systems, Inc.
operating the
Oak Ridge National Laboratory
Oak Ridge Y-12 Plant
under Contract No. DE-AC05-84OR21400
for the
U. S. DEPARTMENT OF ENERGY
Oak Ridge Gaseous Diffusion Plant
Paducah Gaseous Diffusion Plant

DISTRIBUTION OF THIS DOCUMENT IS UNLIMITED

TABLE OF CONTENTS

	<u>Page</u>
LIST OF TABLES.	v
LIST OF FIGURES	vii
ACKNOWLEDGMENTS	ix
ABSTRACT.	xi
I. INTRODUCTION.	1
a. Purpose and Scope	1
b. Previous Studies.	1
c. Analytical Methods.	3
d. Quality Assurance	7
II. LOWER-VESSEL RUBBLE STUDY	8
a. Spherical Rubble Model.	8
b. Optima Fuel Volume Fractions.	10
c. Finite Systems.	13
d. Burnup Analysis	25
III. BENCHMARK CRITICAL EXPERIMENTS.	34
IV. SUMMARY REMARKS	36
V. REFERENCES.	37
APPENDIX: Effect of Rubble Particle Size on Lower-Vessel Models.	38
MICROFICHE: Selected Analyses	

LIST OF TABLES

	<u>Page</u>
Table 1. Performance of the SCALE 27 Group ENDF/B-IV Library on Low-Enriched H ₂ O-Moderated Systems	6
Table 2. U(2.57)O ₂ Spherical-Cell Infinite-Lattice Multiplication Factor vs Fuel Volume Fraction	11
Table 3. U(2.96)O ₂ Spherical-Cell Infinite-Lattice Multiplication Factor vs Fuel Volume Fraction	12
Table 4. Boron Worth for Infinite Lattices of Batch "3" Rubble at Optimum Volume Fraction	14
Table 5. Cell Multiplication vs Temperature.	15
Table 6. Dimensions, Spherical Model	18
Table 7. Dimensions, Lenticular-Fuel Murray Model.	19
Table 8. Dimensions, Lower Vessel Flat Top and Lenticular Fuel Models.	20
Table 9. Results of TMI-2 Lower-Vessel Rubble Studies.	22
Table 10. Supplementary Results on Fissile Inventory and Geometry.	23
Table 11. Infinite Lattice Cell Analyses for Cross Section Generation.	24
Table 12. TMI-2 Soluble Boron History	31
Table 13. K _∞ of Lattice of Batch "3" Rubble with Burnup (TMI-2) . .	32
Table 14. Analysis of Critical Experiments for TMI-2 Benchmarking .	35
Table A1. Summary of Particle Size Study.	40
Table A2. Finite Systems with Optimum Fuel Particle Size.	41
Table A3. Infinite Lattice Cell Analyses for Cross-Section Generation.	42

LIST OF FIGURES

	<u>Page</u>
Figure 1. Cutaway View of Reactor Vessel, Core and Internals . . .	2
Figure 2. Approximation of Core Conditions as Seen by the Quick Look Inspections	4
Figure 3. Spherical Rubble Model	9
Figure 4. Multizone Spherical Model.	16
Figure 5. Lenticular-Fuel Murray Model	17
Figure 6. TMI-2 Plan View Showing Fuel Enrichment.	26
Figure 7. TMI-2 Burnup as of March 19, 1979.	27
Figure 8. TMI-2 Power History, 1978, 1979.	29

ACKNOWLEDGMENTS

The authors wish to recognize the extensive involvement of the TMI-2 Defueling Design Team members D. S. Williams, R. L. Murray, P. S. Kepley and W. C. Hopkins in the definition of the analyses performed in this study. Other members of the Criticality Task Force who contributed substantially to the direction of the study include P. Bradbury, W. E. Austin, G. R. Skillman, R. Smith, F. M. Alcorn, J. R. Worsham, G. M. Jacks, R. L. Rider, C. L. Reid, W. R. Stratton and R. S. Brodsky.

The analyses were reviewed by E. Walker, I. E. Fergus, D. S. Williams and R. L. Murray.

During the conduct of the study, the authors received expert advice on the analyses from L. M. Petrie and N. F. Landers.

M. N. Baldwin and R. Q. Wright provided information on the critical experiments which supplemented the descriptions given in the documents referenced.

The funding support for the study was coordinated by E. M. Collins, W. W. Bixby, H. M. Burton and W. A. Franz.

The careful preparation of the manuscript by Jeanette Hamby is gratefully acknowledged.

ABSTRACT

A bounding strategy has been adopted for assuring subcriticality during all TMI-2 defueling operations. The strategy is based upon establishing a safe soluble boron level for the entire reactor core in an optimum reactivity configuration. This paper presents the determination of a fuel rubble model which yields a maximum infinite lattice multiplication factor and the subsequent application of cell-averaged constants in finite system analyses. Included in the analyses are the effects of fuel burnup determined from a simplified power history of the reactor. A discussion of the analytical methods employed and the determination of an analytical bias with benchmark critical experiments completes the presentation.

I. INTRODUCTION

I.a. Purpose and Scope

At a meeting on February 3, 1984, the TMI-2 Criticality Task Force decided to take a "bounding" approach in defining a concentration of soluble boron that would maintain the core in a shutdown condition for all fuel removal operations. This decision led to a series of requests by the TMI-2 Defueling Design Team for supporting analyses to be performed by the Nuclear Engineering Applications Department (NEAD). Generally, the analyses served two functions:

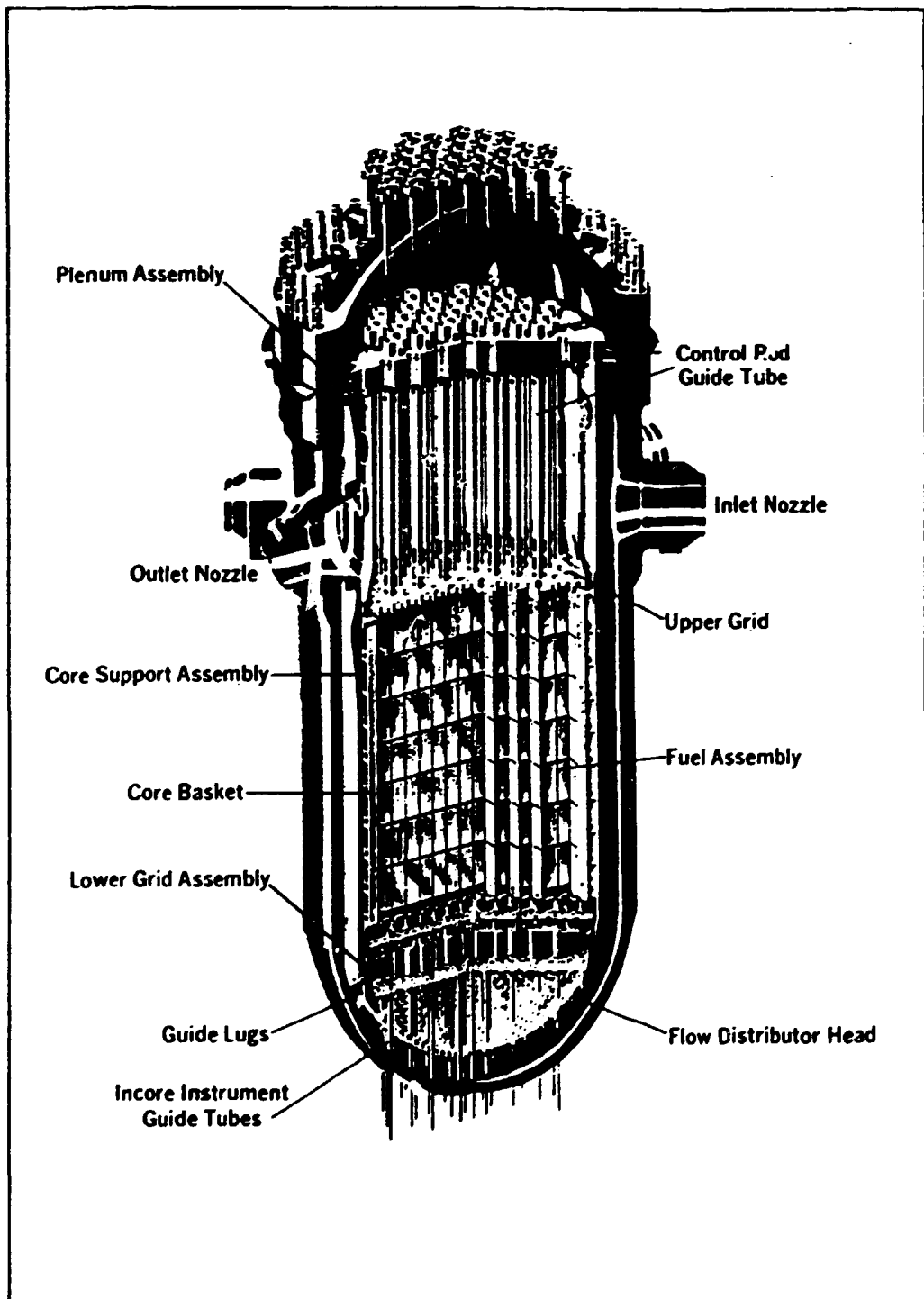
1. establish system multiplication factors for the fuel rubble in optimum reactivity configurations, and
2. establish the analytical bias for the performance of the NEAD computer programs and data libraries in the analysis of low-moderated, highly-borated systems.

The purpose of this memorandum is to report these analyses in a formal document. The scope of the report is limited to the technical aspects of the study. The rationale for determining which systems were to be analyzed was developed by the Criticality Task Force and Defueling Design Team. The technical bases for this rationale were derived from the results of previous studies.

I.b. Previous Studies

A cut-away view of the reactor vessel, internals and fuel assemblies in the as-built condition is shown in Figure 1. Immediately after the accident, the high level of radiation from fission products in the reactor coolant indicated that the fuel assemblies had sustained substantial damage. However, the extent of core disruption and fuel displacement could not be directly observed. A core damage assessment performed by the Babcock & Wilcox Company predicted severe damage to the upper central region of the reactor. This information was applied by Westfall et al.¹ in the analysis of various disrupted core models for the President's Commission on Three Mile Island. Their general conclusion was that the damaged core with a coolant boron concentration of 3180 WPPM has a system multiplication factor of approximately 0.86.

Subsequent to the disrupted core study, a more general analysis of the effect of oxide fines on the neutron multiplication factor was performed by Thomas.² This study involved uniform $U(3)O_2$ and $U(3)_3O_8$ water mixtures at various oxide densities and soluble boron levels. The oxide fines were considered in geometries which included both homogeneous single units and arrays of fuel assemblies with the fines interspersed between the fuel pins.



Babcock & Wilcox

Figure 1. Cutaway View of Reactor Vessel, Core and Internals

An extensive series of analyses to support TMI-2 recovery operations through head removal was performed by the Babcock & Wilcox Company and reported in 1982 by Worsham et al.³ One major result of this study is the postulation of a maximum credible damage model which has a system multiplication factor of approximately 0.94. This model includes various assumptions which maximize the reactivity effect of fuel particle size, geometry and location. The authors recognized that a "more realistic value of k_{eff} is less than 0.902."

The "Quick Look" series of reactor core inspections were completed in 1983. The results of the videotape analyses are reported in Reference 4, from which Figure 2 is extracted. In support of the Criticality Task Force, W. R. Stratton, criticality consultant to General Public Utilities, requested a new series of disrupted core analyses to incorporate the "Quick Look" findings. Parametric variations investigated in these analyses included ^{235}U enrichment, the system geometry, the fuel pin lattice pitch, the U_0_2 and U_3O_8 volume fractions and the soluble boron content of the coolant. The study was recently reported by Thomas.⁵ Additional ultrasonic observations of the core made during the performance of the study indicated that very few of the fuel assemblies remain intact above the 14" thick rubble bed shown in Figure 2. Therefore these analyses modeled a series of fuel assembly heights with the balance of the core represented as rubble distributed above, below and interspersed within the fuel assemblies. Since there is no direct correspondence in analytical models, exact comparisons with the earlier disrupted core analyses done at Oak Ridge and by Babcock & Wilcox cannot be drawn. However, the recent analysis of the 7 foot high core at 3500 WPPM boron and with a uniform slurry of U_3O_8 rubble results in a system multiplication factor of 0.862, in good agreement with the earlier Oak Ridge results. When the fixed absorbers are removed from the core and all of the rubble is represented as a bed of U_0_2 pellets at optimum volume fraction on top of the core, the system multiplication factor is 0.949, in reasonable agreement with the Babcock & Wilcox value for their maximum credible damage model. Thus, there is a good basis for believing that the reactivity mechanisms associated with the current status of the reactor core are well understood.

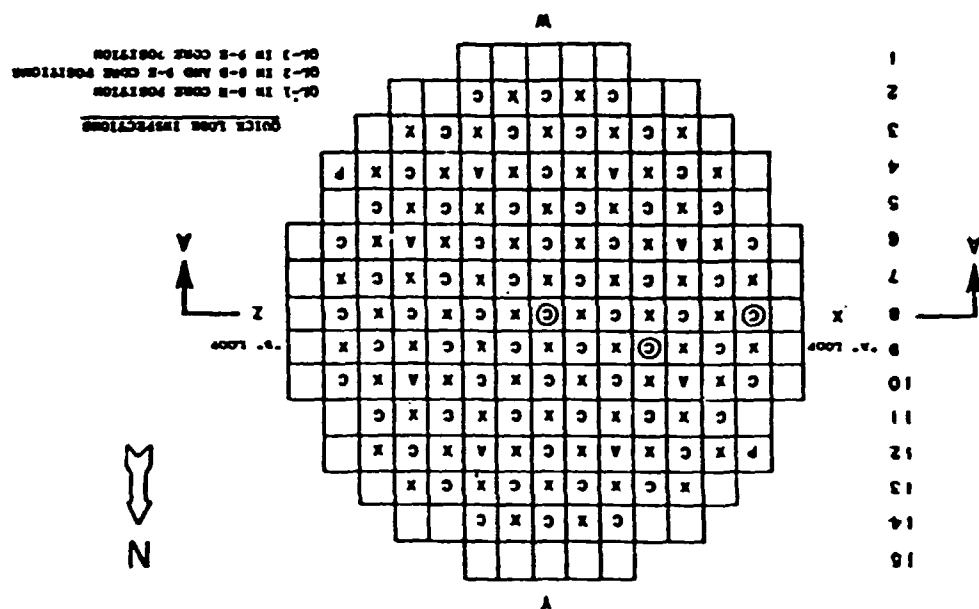
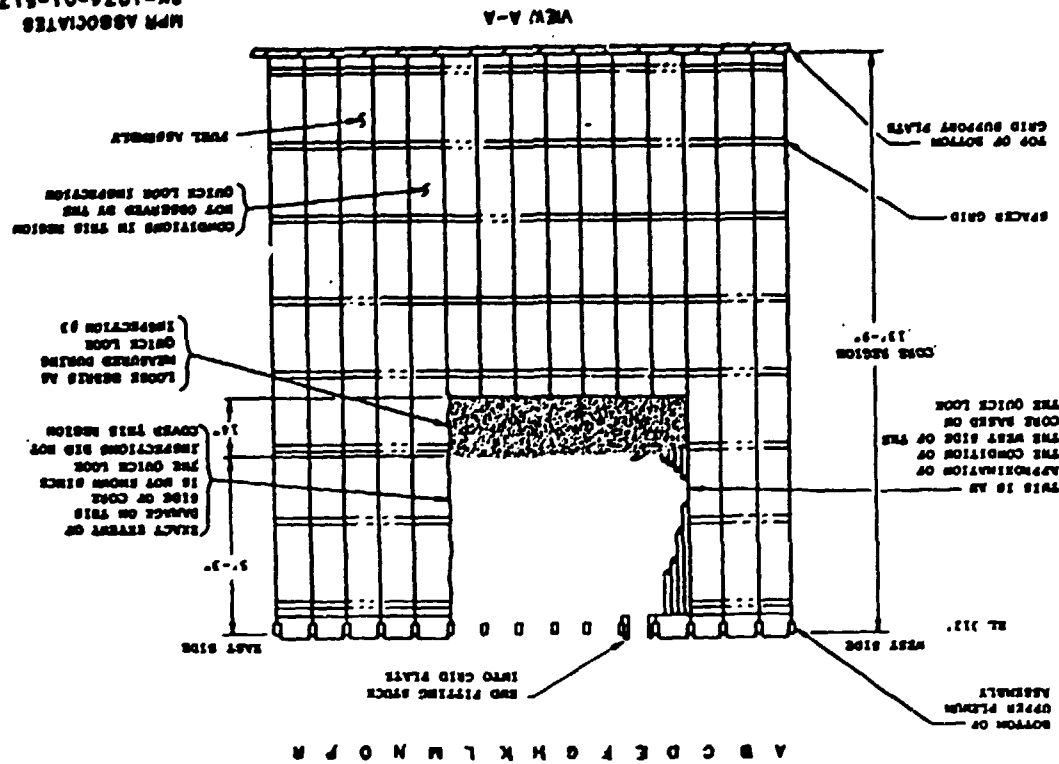
The understanding of these reactivity mechanisms and the potential for fuel rubble accumulation in the lower-vessel region led to the characterization of the optimum reactivity configurations analyzed in the present study.

I.c. Analytical Methods

The computer programs and cross section data applied in this study were from the SCALE system.⁶ This system was developed for the NRC to perform standardized criticality safety, radiation shielding and heat transfer analyses. The system includes control modules which interpret the materials and geometry information in the user-specified input to perform cross-section processing and systems end-analysis. The major SCALE functional modules applied in this study were:

Figure 2. APPROXIMATION OF CORE CONDITIONS AS SEEN BY THE QUICK LOOK INSPECTIONS

MEA. 0
8K-1074-01-817
MHP ASSOCIATES



OKNL-DWC 85-16541

SUPERDAN - used to determine Dancoff factors for fuel pins and pellets in lattice cell geometries by applying numerical integration,

NITAWL-S - used to perform resonance shielding of cross section data by applying the Nordheim Integral Technique,

XSDRNPM - used to perform cell-averaging of cross section data and to determine multiplication factors for systems having one-dimensional variation through the application of the discrete-ordinates transport equations,

KENO-V.a - used to determine multiplication factors for multi-dimensional systems through the application of the Monte Carlo technique,

and **ORIGEN-S** - used to determine fuel burnup, actinide transmutation, and fission product buildup and decay through the application of the matrix exponential expansion technique.

Each of these major computer programs is described in the SCALE system documentation. The SCALE 27 group, ENDF/B-IV neutron cross section library was applied in the criticality analyses. This library was supplemented with ENDF/B-V data for certain of the fission products in the burnup analyses. The SCALE 123 group GAM-THERMOS library was applied in some of the benchmark analyses for comparison with the performance of the ENDF/B data.

A summary of the performance of the SCALE 27 group ENDF/B-IV library in the analysis of low-enriched, water-moderated systems is given in Table 1. The systems are ordered, left to right, on the basis of increasing moderation. Two aspects of the experiments should be noted and commented upon. The UO_2 pin lattices were designed to simulate a 3×1 array of fuel assemblies separated by water gaps and absorber plates. Also, the uranium metal pin lattice experiments were performed with various patterns of water gaps created by lattice vacancies. The fixed absorber plates, as well as the fluorine, are not considered to have a significant effect upon the neutron energy spectrum. However, for any particular experiment, the additional water due to lattice vacancies will increase the $H/^{235}U$ atom ratio above the values shown in Table 1.

Given these qualifications, the results for all 119 critical experiments support two general observations.

1. The average values for the calculated system multiplication factors vary from somewhat more than 1% Δk low for the dryer systems to approximately critical for the well-moderated systems.
2. The maximum deviation from the average value for any particular set of experiments is quantitatively on the order of the 3 standard deviation uncertainty associated with a 99.7% confidence level.

Table 1. Performance of the SCALE 27 Group ENDF/B-IV Library on Low-Enriched, H_2O -Moderated Systems

Analytical Reference	8	7	7	8	8
Number of Experiments	25	35	35	14	10
Fuel Enrichment & Geometr,	U(4.89) Metal Pin Lattice	U(4.29) O_2 Pin Lattice	U(2.35) O_2 Pin Lattice	U(4.89) Metal Pin Lattice	U(4.89) O_2F_2 Single Units
Moderator	H_2O	H_2O	H_2O	U(4.89) O_2F_2 Solution**	U(4.89) O_2F_2 Solutions
Fixed Absorbers	None	Yes*	Yes*	None	None
Minimum k_{eff}	0.985±0.003	0.974±0.004	0.986±0.004	0.985±0.003	0.991±0.003
Maximum k_{eff}	0.994±0.003	0.997±0.004	1.004±0.004	1.006±0.002	1.005±0.002
Average k_{eff}	0.989	0.988	0.994	0.995	0.997
$H/^{35}U$ Atom Ratio, Cell***	78-237	246	398	209-471	524-1099

*SS-304L, SS+B, Cd, Boral, Cu, Zr, Al

**Uranium at 300 g/l

***Minimum bounding values assuming uniform lattices

In summary, the results indicate a positive trend with neutron moderation and their distribution is consistent with expected statistical behavior.

I.d. Quality Assurance

Analyses constituting this study were performed in compliance with the quality assurance program of the Computing and Telecommunications Division of Martin Marietta Energy Systems, Inc. Computational software and data libraries are quality assured through the Configuration Control Management System. Individual case input and output records are retained for future reference and/or reproducibility.

II. LOWER-VESSEL RUBBLE STUDY

II.a. Spherical Rubble Model

In all of the analyses performed under this study, the fuel was represented as a homogeneous medium for which the neutronic data corresponds to a lattice of spherically shaped fuel pellets. The features of this rubble model are summarized in Figure 3. From the reactivity viewpoint, the model includes three conservative assumptions.

1. The only materials in the model are UO_2 pellets and borated water. Thus, the negative reactivity effects due to the possible presence of fuel clad, fixed absorbers and structural materials are ignored.
2. The preservation of the design pellet surface-to-mass (S/M) ratio in the specification of the spherical pellet volume enhances the resonance shielding effect on the ^{238}U cross sections. On the basis of the "Quick Look" observations, this is an upper limit on the actual rubble particle size.
3. For each soluble boron concentration, a search was performed to determine the lattice pitch (or, correspondingly, fuel volume fraction) which gives a maximum value of the infinite lattice multiplication factor.

These three assumptions tend to maximize the reactivity worth of the neutronic constants processed for the rubble media. For example, in the range of 3500-4500 WPPM soluble boron, the presence of zircalloy clad in the model would reduce the maximum lattice cell multiplication factor by approximately 2% Δk . Consideration of the heterogeneous UO_2 pellet-water mixture rather than a homogeneous U_3O_8 -water slurry increases the multiplication factor by 3% Δk . It should be noted that a model based upon an unclad fuel pin of infinite height and design diameter would be worth approximately 1% Δk more than the spherical pellet model applied in this study. However, the spherical pellet model corresponds to an optimum credible arrangement of the fuel pellets, considering a random fuel reassembly following core disruption.

The neutronic constants for the rubble media were obtained with an automated procedure executed with the SCALE system control module CSAS1X. Two major steps in the procedure involve resonance shielding and cell averaging. The twelve-sided, dodecahedral unit cell applied in the NITAWL-S resonance-shielding analysis is represented by the Dancoff factor as determined with the SUPERDAN module. The equivalence between this unit cell and the two-region, spherical unit cell applied in the subsequent XSDRNPM cell-averaging calculation comes from the preservation of the fuel volume fraction. As derived from Cundy and Rollett,⁹ the fuel volume fraction in the dodecahedral cell is given by

ORNL-DWG 85-16542

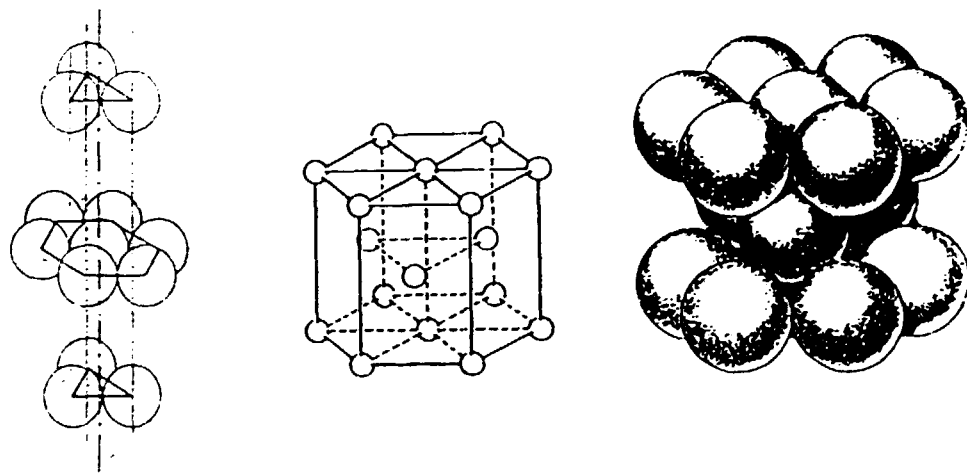


Figure 3. Spherical Rubble Model

1. PELLET RADIUS = 0.5362 CM, PRESERVES S/M RATIO OF ACTUAL PELLET.
2. DODECAHEDRAL UNIT CELL, EACH SPHERE HAS 12 NEIGHBORS FOR DANCOFF FACTOR.
3. XSDRNPM TWO-REGION SPHERICAL CELL, OUTER CELL RADIUS = 0.55267*PITCH.
4. CELL-AVERAGED CROSS SECTIONS IN KENO RUBBLE.

$$(Fuel VF)_{DC} = \frac{4\sqrt{2}}{3} \pi (r_1/P)^3, \quad (1)$$

where r_1 is the pellet radius and P is the lattice pitch. For the two-region, spherical cell with outer radius r_2 , the fuel volume fraction is given by

$$(Fuel VF)_{SC} = (r_1/r_2)^3. \quad (2)$$

Conserving the fuel volume fraction as expressed in equations (1) and (2) yields

$$r_2 = 0.55267 P. \quad (3)$$

In specifying the input for the CSAS1X control module, the lattice pitch for the desired fuel volume fraction is obtained from equation (1). Then CSAS1X determines r_2 for the XSDRNPM cell analysis by equation (3).

As applied in SCALE, XSDRNPM uses a standard prescription for discrete-ordinates quadrature type and order, scattering expansion order, spatial mesh specifications, and convergence criteria. For pin lattice geometries which can be represented explicitly in KENO V.a, comparisons have been made between the use of neutronic constants which have been cell-averaged in XSDRNPM according to this prescription and neutronic constants processed by NITAWL-S for the fuel pins. Thus, in both cases the end analysis was done with KENO V.a, one with cell-averaged constants, the other with the fuel pins represented explicitly. The good agreement in the results indicates the effectiveness of the XSDRNPM cell-averaging procedure. It should be noted that the KENO V.a geometry package cannot represent the dodecahedral cell boundary explicitly and thus the cell-averaging of neutronic constants was a necessity for this model.

II.b. Optimal Fuel Volume Fractions

A number of CSAS1X analyses were performed to establish the optimum fuel volume fraction in the spherical rubble model as a function of soluble boron content of the coolant. Initially, these analyses were done for the average fuel enrichment, 2.57 weight percent ^{235}U , in the reactor core. A uniform mixture of the three fuel batches was assumed for the rubble regions in the disrupted core analyses reported by Thomas.⁵ The results for soluble boron levels ranging from 3500 to 5500 WPPM are listed in Table 2. Subsequent analyses were performed for the batch 3, 2.96 weight percent ^{235}U , fuel modeled in the lower-vessel rubble study. These analyses are summarized in Table 3. Several observations can be drawn from the results.

Table 2. $^{235}\text{U}(2.57)\text{O}_2$ Spherical-Cell Infinite-Lattice Multiplication Factor^a
vs. Fuel Volume Fraction

Soluble Boron (WPPM)	3500	3500	4500	4500	5500
Temperature (°K)	273	283	273	283	283
<u>Fuel Fraction</u>					
0.50	0.9826	-	0.9267	-	-
0.55	0.9958	0.9953	0.9479	-	-
0.56	-	0.9968	-	-	-
0.57	-	0.9978	-	-	-
0.58	0.9988**	0.9982	0.9556	-	-
0.59	-	0.9983**	-	-	-
0.60	0.9985	0.9980	0.9601	-	-
0.61	0.9978	-	0.9611	0.9606	-
0.62	0.9975	0.9980	0.9616**	0.9611**	-
0.63	0.9972	-	0.9618**	0.9613**	0.9291
0.64	0.9955	-	0.9616	0.9611	0.9303
0.65	0.9935	0.9929	0.9611	0.9606	0.9310
0.66	-	-	-	-	0.9313**
0.67	0.9882	-	0.9588	-	0.9312
0.68	-	-	-	-	0.9308
0.69	0.9815	-	0.9550	-	0.9300

^a As determined by XSDRNPM with the 27 group ENDF/B-IV library in the CSAS1X SCALE Sequence.

^{**} Maximum value calculated.

Table 3. $\text{U}(2.96)\text{O}_2$ Spherical-Cell Infinite-Lattice Multiplication Factor^a
vs Fuel Volume Fraction

Soluble Boron (WPPM)	3500	4200	4350	4750	4800
<u>Fuel Fraction</u>					
0.56	1.03821	-	-	-	-
0.57	1.03859 ^{**}	-	-	-	-
0.58	1.03844	1.00921	-	-	0.98580
0.59	1.03794	1.00986	-	0.98925	0.98874
0.60	1.03711	1.01166	1.00613	0.99173	0.98997
0.61	1.03634	1.01167 ^{**}	1.00635 ^{**}	0.99236	0.99083
0.62	1.03592	1.01114	1.00605	0.99278	0.99115
0.63	1.03404	1.01037	1.00549	0.99279 ^{**}	0.99123 ^{**}
0.64	-	-	-	0.99180	0.99087
0.65	-	-	-	-	0.99021

^a As determined by XSDRNPM with the 27 group ENDF/B-IV library (283°K) in the CSAS1X SCALE Sequence.

^{**} Maximum value calculated.

1. The optimum fuel volume fraction varies from approximately 0.57 to 0.66 over the soluble boron range of 3500 to 5500 WPPM.
2. For a given boron level, the multiplication factor varies slowly with the fuel volume fraction. Near the peak, a volume fraction variation of one figure in the second decimal place results in a multiplication factor variation of a few figures in the fourth decimal place.
3. For the variations in fuel enrichments and fuel temperatures analyzed, there appears to be no significant variation in the location of the peak values of the multiplication factors.

It should be noted that the source term and point flux convergence criteria specified by the CSAS1X sequence for XSDRNP are both 10^{-4} . Thus, the values of the multiplication factors in Tables 2 and 3 are accurate to only one figure in the fourth decimal place of $\sim 0.1\% \Delta k/k$. A brief investigation with tighter convergence criteria showed consistently higher multiplication factors and no difference in the variation with fuel volume fraction. The optimum fuel volume fractions shown in Table 3 were the values applied in the lower-vessel rubble study. Tables 4 and 5 list the results of parametric variations performed with lattice cell analyses to demonstrate the differential worth of soluble boron and fuel temperature upon the multiplication factor.

II.c. Finite Systems

Each of the models applied in the lower-vessel study included fuel-rubble and borated-water regions contained in an 8-inch-thick, SS-304 reflector representative of the hemispherically shaped lower vessel shown in Figure 1. The actual presence of steel members interior to the vessel (such as the lower grid and the flow distributor) was ignored as a conservative approximation.

The models characterized the fuel region as having one of three geometry shapes: spherical lenticular or lens shaped, and semi-lenticular or flat-top. General sketches of the models are shown in Figures 4 and 5. Dimensions for the various cases are given in Tables 6, 7 and 8. The volume of a lenticular region is given by

$$V = 2\pi h^2 (r - h/3),$$

where h is the region's half-height and r is the radius of curvature of the outer surface. The fuel volume of the flat top model is one-half of this value. For a given fuel volume, leakage considerations from elementary reactor theory predict that the spherical fuel geometry is the most reactive. The lenticular and flat-top fuel geometries produce progressively more leakage and therefore are less reactive. Thus, the

Table 4. Boron Worth for Infinite Lattices of Batch "3" Rubble at
Optimum Volume Fraction

Boron Level (WPPM)	Fuel Volume Fraction	Multiplication Factor	Boron Worth (WPPM/1% Δk)
4800	0.63	0.9912	313
4750	0.63	0.9928	291
4200	0.61	1.0117	260
3500	0.57	1.0386	

Table 5. Cell^{*} Multiplication vs Temperature

Temperature Degrees			Multiplication Factor**	$\Delta k/10^{\circ}\text{K}$
K	C	F		
323	50	122	0.99064	0.00052
313	40	104	0.99116	0.00054
303	30	86	0.99170	0.00054
293	20	68	0.99224	0.00056
283	10	50	0.99279	0.00055
273	0	32	0.99335	

* U(2.96)O₂-Borated H₂O (4750 WPPM) Spherical Model Bubble Fuel Cell.

** XSDRNPM

ORNL-DWG 85-16543

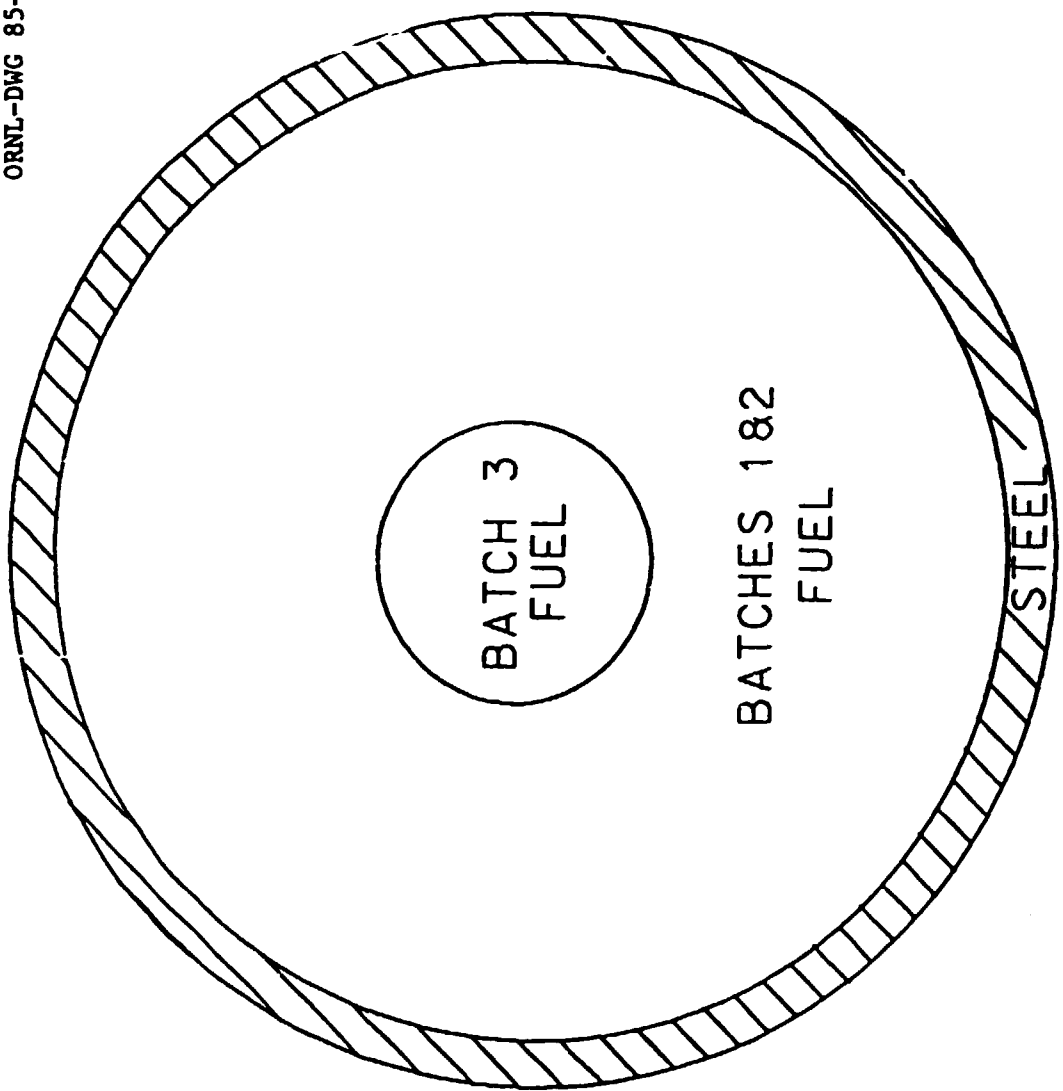


Figure 4. Multizone Spherical Model

ORNL-DWG 85-16544

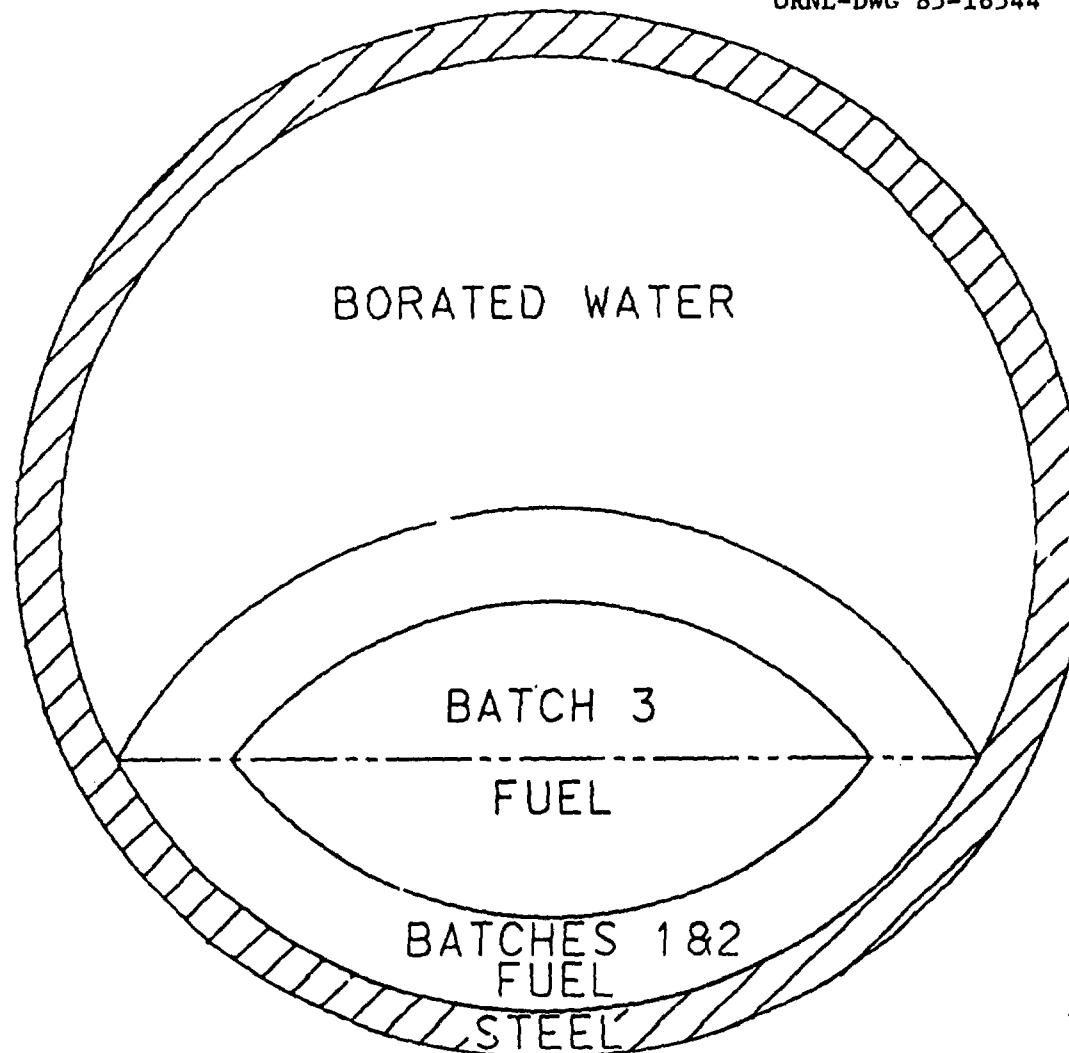


Figure 5. Lenticular-Fuel Murray Model

Table 6. Dimensions, Spherical Model

Material Zone *	Case:	A, A'	C	Outer Radius (cm)		
				C'	C"	D, D'
Batch "3" (2.96% Fuel		106.26	74.09	74.09	74.09	107.41
Batches "1" & "2" (2.34% Av.) Fuel		152.4	-	-	-	154.04
Borated H ₂ O		-	-	76.63	79.17	-
SS-304		172.72	94.41	96.95	99.49	174.36

* Zones listed in sequence of inner to outer.

Table 7. Dimensions, Lenticular-Fuel Murray Model

Material Zone*	Case:	<u>Half-Height (cm)</u>		<u>Radius of Curvature (cm)</u>	
		B, B'	D", D""	B, B'	D", D""
Batch "3" (2.96%) Fuel		79.9565	81.4140	151.777	151.777
Batches "1" & "2" (2.34%) Fuel		114.673	116.754	217.678	217.678

*Outer radius of 8-inch-thick SS-304 spherical reflector was 237.998 cm for all cases. Half-heights are measured from the bottom center of the inner surface of this reflector. Borated H₂O filled the non-fueled region interior to the spherical reflector.

Table 8. Dimensions, Lower Vessel Flat Top and Lenticular Fuel Models*

Case	Fuel Shape	Fuel Height (cm)	Borated H ₂ O Thickness (cm)
F	Flat Top	171.45	46.228
F'	"	158.75	58.928
F"	"	97.94	119.738
H	"	97.94	119.738
H'	"	78.45	139.228
H"	"	54.35	163.328
H'''	Lenticular	37.91 (half-height) 217.678 (radius of curvature)	179.768 (maximum) 141.858 (minimum)

* Model consists of an 8-inch-thick hemispherical shell (inner radius 217.678 cm, outer radius 237.998 cm) of SS-304 containing the fuel covered by borated H₂O. The fuel heights are measured from the bottom center of the inner surface of the steel shell.

idealized spherical fuel geometry is the most conservative from the criticality safety standpoint; while the other models are less conservative but more realistic. Also, it should be noted that the spherical model is amenable to highly-precise analysis with the one-dimensional discrete-ordinates code, XSDRNPM.

The primary results for the finite system analyses are listed in Table 9. Supplementary results for various configurations of the batch "3" rubble are given in Table 10. For those cases which are essential to the determination of the operational and safety limits on soluble boron level during defueling, microfiche copies of the computer listings have been included in this report. Also included are microfiche copies of the infinite lattice cell analyses used to generate the fuel rubble cross sections. The conditions on the cell analyses and the microfiche identifiers are cross referenced in Table 11. Five results of the finite systems studies are summarized.

1. Reflector Worth - Sixty assemblies of batch "3" fuel were analyzed with various combinations of stainless steel and borated water reflectors. At 4750 WPPM boron, the results of Cases C, C' and C" in Table 9 show that, for these systems, stainless steel is a better reflector than borated water. A similar study showed the same result for water at 3500 WPPM boron.
2. Base Case - A two-fuel-zone, eight-inch stainless steel-reflected sphere is reported as Case A in Table 9. This represents the actual inventory with the batch "3" (2.96% enriched) fuel centered in a mixture of the lower-enriched batch "1" and "2" (2.34% average enrichment). In addition to the conservatism in the rubble characterization discussed above, this configuration is conservative with regard to fuel inventory, fuel arrangement and fuel geometry. Also, this case assumes beginning-of-life fresh fuel and thus does not account for any burnup.
3. Fuel Inventory Worth - Comparison of Cases A and C in Table 9 shows that the additional worth of batches "1" and "2" is 0.5% Δk when treated as an average enrichment. Comparison of Cases E and F in Table 10 shows a minimum leakage of 2% Δk for the finite, steel-reflected systems. Also in Table 10, comparison of Cases F and F" shows a 2.4% Δk effect in going from 177 to 66 assemblies. Comparison of Cases H and H" shows a 5.8% Δk effect in going from 60 to 20 assemblies in the "flat top" configuration shown in Figure 4.

Table 9. Results of TMI-2 Lower-Vessel Rubble Studies

Case	Boron (WPPM)	Inventory	Model	Code	Multiplication Factor	Microfiche Identifier & Date	
A	4750	60 Assy "3" 117 Assy "1" & "2" (Figure 4)	3 Zone Sphere	XSDRNP M KENO V.a	0.9716 0.9723 ± 0.0014	JRKTMIF2 JRKTMIK2 08/27/84 08/22/84	
A'	4750	60 Assy "3 Burned" 117 Assy "1" & "2"	"	XSDRNP M KENO V.a	0.9537 0.9548 ± 0.0016	JRKTMIB JRKTMIKB 08/27/84 08/24/84	
B	4750	60 Assy "3"	3 Zone Lenticular Fuel Murray Model (Figure 5)	KENO V.a	0.9685 ± 0.0020	JRKTMIK	09/27/84
B'	4750	60 Assy "3 Burned" 117 Assy "1" & "2"	"	"	0.9520 ± 0.0018	JRKTMIKB	10/08/84
C	4750	60 Assy "3"	2 Zone Sphere	XSDRNP M	0.9672	-	-
C'	4750	"	3 Zone Sphere	"	0.9650	-	-
C"	4750	"	3 Zone Sphere	"	0.9642	-	-
D	4200	60 Assy "3" 117 Assy "1" & "2"	3 Zone Sphere	"	0.9884	JRKTMIF	10/01/84
D'	4200	60 Assy "3 Burned" 117 Assy "1" & "2"	"	"	0.9720	JEKTMIBB	10/01/84
D"	4200	"	3 Zone, Lenticular Fuel Murray Model	KENO V.a	0.9688 ± 0.0016	JRKTMIKF	10/08/84
D'''	4350	"	"	"	0.9646 ± 0.0017	JRKTMIKG	10/08/84

Table 10. Supplementary Results on Fissile Inventory and Geometry

Case	Boron (WPPM)	Inventory	Model	Code	Multiplication Factor
E	4800	Assy "3" Rubble	Infinite Lattice (Figure 3)	XSDRNPM	0.9912
F	4800	177 Assy "3"	Lower Vessel Flat Top	KENO V.a	0.9693±0.0030
F'	4800	166 Assy "3"	"	"	0.9657±0.0024
F"	4800	66 Assy "3"	"	"	0.9452±0.0029
G	3500	Assy "3" Rubble	Inrinite Lattice	XSDRNPM	1.0386
H	3500	60 Assy "3"	Lower Vessel, Flat Top	KENO V.a	0.9877±0.0031
H'	3500	40 Assy "3"	"	"	0.9752±0.0030
H"	3500	20 Assy "3"	"	"	0.9294±0.0031
H'''	3500	20 Assy "3"	Lower Vessel, Lenticular Shape	"	0.9636±0.0029

Table 11. Infinite Lattice Cell Analyses^{*} for Cross Section Generation

Fuel Enrichment (wt % ^{235}U)	Boron Level (WPPM)	Fuel Volume Fraction	Multiplication Factor	Microfiche Identifier & Date
2.96	4750	0.63	0.9923	JRKTMIX2 07/18/84
2.34	4750	0.63	0.9254	JRKTMIX3 07/18/84
2.67	4750	0.63	0.9747	JRKTMIXB 08/01/84
2.96	4200	0.61	1.0111	JRKTM12F 09/10/84
2.34	4200	0.61	0.9439	JRKTM13F 09/10/84
2.67	4200	0.61	0.9929	JRKTM1BF 02/14/85 (Rerun)
2.67	4350	0.61	0.9881	JRKTM1BG 10/08/84
2.34	4350	0.61	0.9382	JRKTM13G 10/08/84

^{*}All of the analyses were done at a temperature of 293°K (68°F). The 2.96 and 2.67% enrichments are the batch "3" fuel in the unburned and 2535 MWD/MTU burned conditions. The 2.34% enrichment represents an average of batches "1" and "2" in the unburned condition.

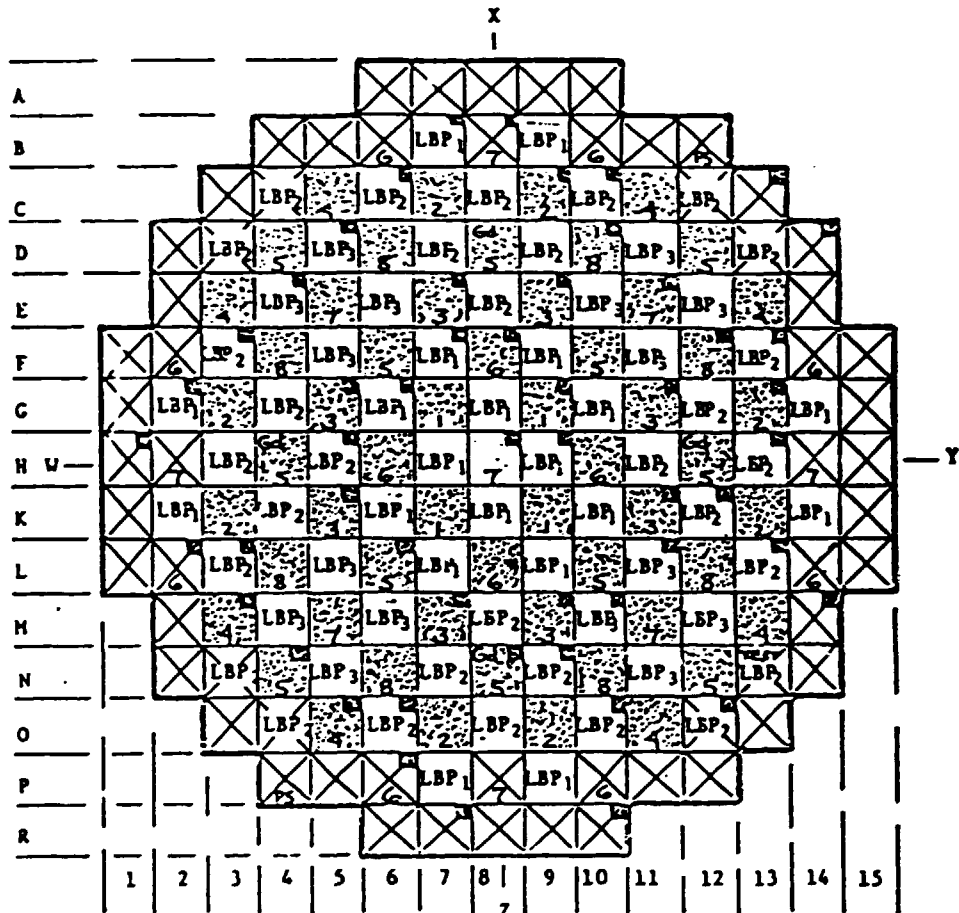
4. Geometry Shape Worth - Comparison of Cases A and B shows a 0.3% Δk reduction in going from the hypothetical spherical model to the more-plausible lenticular shape model shown in Figure 5. Additional comparisons: A'-B' and D'-D" yield the same value. For the 20 assemblies considered in Cases H" and H'", flattening the top of the lenticular model reduces the multiplication factor by 3.4% Δk . Thus the fissile geometry shape has a significant effect upon small inventories.
5. Boron Level Worth - Comparison of Cases A' and D' shows 1.83% Δk increase in reactivity in going from 4750 to 4200 WPPM boron. Cases A and D show an effect of 1.68% Δk . These values predict a boron reactivity worth of approximately 300 to 330 WPPM/1% Δk . The infinite lattice data in Table 4 predict a boron worth in agreement with these values and also demonstrate a decreasing boron worth with increasing boron level.

II.d. Burnup Analysis

A limited, simplified reactor burnup analysis was performed to determine the reactivity effect of ^{235}U depletion, actinide transmutation and fission product buildup and decay. Using standard light-water-reactor design and fuel management procedures, the Babcock & Wilcox Company has calculated an overall burnup worth of -2.5% $\Delta \rho$ for the damaged core shortly after the accident, which occurred on March 28, 1979. This study is summarized in Table 3.1, page 3-31 of reference 3.

A detailed burnup analysis over the power history of each of the 177 fuel assemblies would be beyond the scope of the present study. A plan view of the core is shown in Figure 6. As noted previously, comparison of Cases A and C in Table 9 shows that batches "1" and "2" are worth only 0.5% Δk when added to batch "3" in the most-reactive configuration. Therefore, this burnup analysis was limited to the batch "3" fuel. Several steps were taken to simplify the definition of the burnup analysis.

1. An average batch "3" assembly burnup was developed from information supplied by the Defueling Design Team. Figure 7 shows assembly burnups as measured¹⁰ by GPU on March 19, 1979. At the time of the accident, the average core burnup was 3165 MWD/MTU.¹⁰ The data in Figure 7 was used to determine batch "3" average and core average values for March 19, 1979. A batch "3" average burnup of 2535 MWD/MTU was obtained for the time of the accident by scaling the March 19th value on the basis of the core average burnup for the two dates.



<u>²³⁵U enrichment</u>	<u>No. assemblies</u>	<u>LBP loading</u>	<u>BuC enrich., wt %</u>
<input checked="" type="checkbox"/>	1.98	56	LBP ₁ 1.43
<input type="checkbox"/>	2.64	61	LBP ₂ 1.26
<input checked="" type="checkbox"/>	2.96	60	LBP ₃ 1.09

Figure 6. TMI-2 Plan View Showing Fuel Enrichment

ORNL-DWG 85-16546

—CARRIER PERFORMANCE DATA DURING SCHEDULE 1
PLANE: JETSETT CRISTAL PAL 7 MILE ISLAND 2
TIME: 10 AM 20 MONTH 03 DAY 14 HOUR 06 MINUTE 18 SEC ESE
TAKED DATE: 05/08/78

ASSEMBLY HUMMERS (HUMMINGBIRDS) - 1977-84

Figure 7. TMI-2 Burnup as of March 19, 1979

2. A simplified exposure history was developed for the batch "3" fuel on the basis of the average burnup of 2535 MW/MTU. A plot of the average daily reactor power is given in Figure 8. The average core exposure was 94.6 effective full power days.¹⁰ The simplified exposure history consists of two fuel burns (45.2 days and 49.4 days) at a full power of 26.8 MW/MTU to produce the average batch "3" burnup. The burn periods are separated by a down time of 27 days. This exposure history is conservative with regard to ^{235}U depletion.
3. The soluble boron history for the TMI-2 reactor is given in Table 12. This data was weighted by the power history to obtain average values of 1330.3 WPPM boron for the first burn period and 1093.9 WPPM boron for the second burn period.

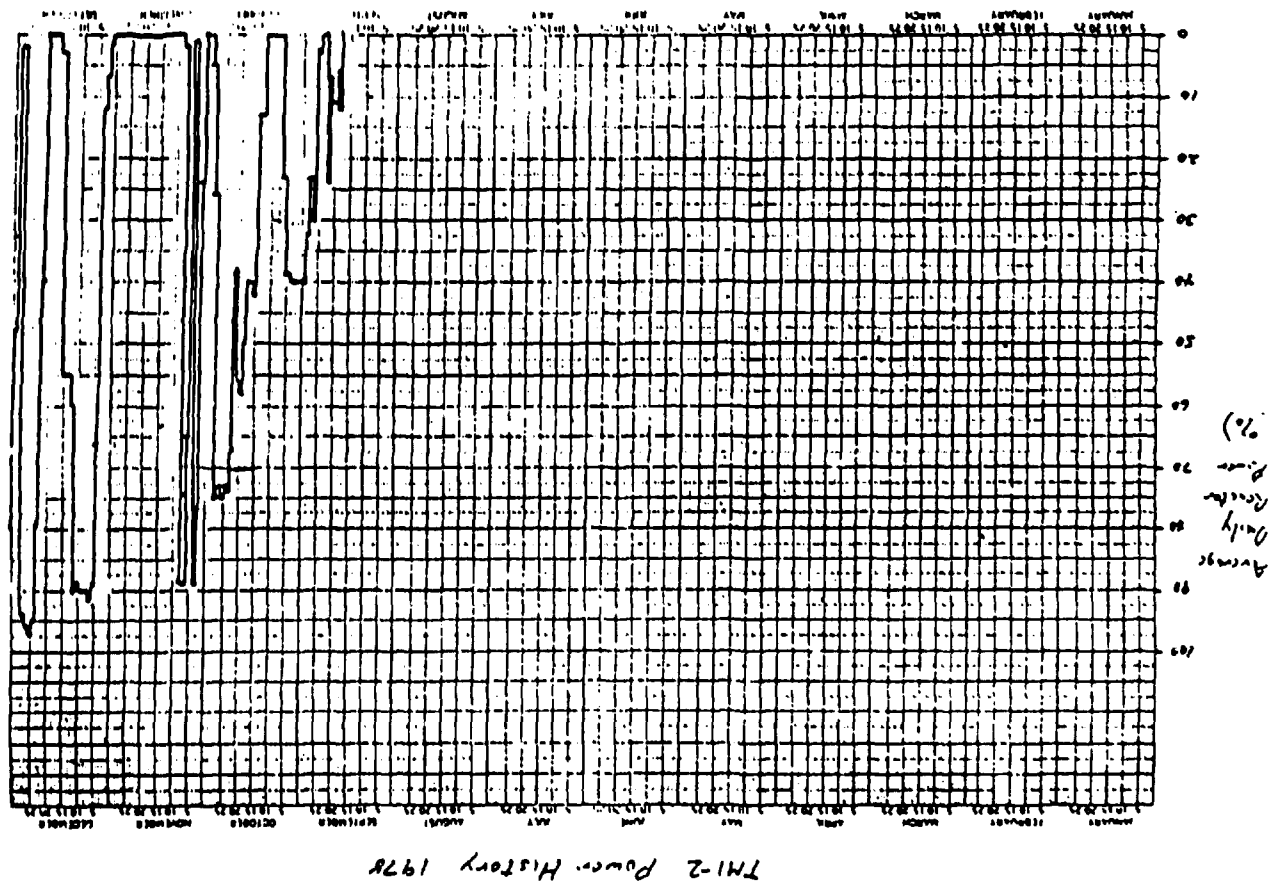
These conditions define the simplified exposure history for the batch "3" fuel assemblies. The burnup analysis was performed for the fuel pin lattice according to the design specifications.¹ Operating conditions included an average fuel temperature of 1000 Kelvin, a water temperature of 579 Kelvin and a water density of 0.7147 g/cm³. The analysis was performed with the SAS2 sequence in the SCALE system.⁶ This sequence applies NITAWL-S and XSDRWPM for cross section processing and ORIGEN-S for the burnup analysis. ENDF/B-V data for various isotopes of lanthanum, cerium, samarium, europium, promethium, neodymium, and praseodymium were used to supplement the SCALE 27 group ENDF/B-IV neutron cross section library.

Subsequent to the second burn period, the radiative decay of the actinides and fission products was determined for a period of 2075 days, the time interval between March 28, 1979 and December 1, 1984. Based on the advice of the Defueling Design Team as to which of the important actinides and fission products are considered to still be in the fuel pellets, the fresh fuel composition was modified to reflect the December 1st concentrations. In order to show the differential worth of the various isotope changes, the spherical rubble model was analyzed with the soluble boron at 4750 WPPM and a room temperature value of 293 Kelvin. The results of these analyses are summarized in Table 13. Twenty-nine actinide and fission product isotopes were included in the most comprehensive calculation, Case 9. Based on these analyses, the overall batch "3" burnup has a potential worth of 1.76 Δk .

The December 1, 1984 fuel composition was applied for the batch "3" fuel in Cases A', B' and C' of Table 9. Comparison with Cases A, B and C indicates burnup worths of 1.79, 1.65 and 1.64% Δk_{eff} , depending on finite system model and soluble boron loading. These values are consistent with that given by the infinite lattice analyses. They are also well within the value of 2.5% $\Delta \mu$ determined by the Babcock & Wilcox Company for the full core at the time of the accident, noted previously.

29

FIGURE 6. THI-2 Power History, 1978



ORNL-DMG 85-16547

ORNL-DWG 85-16548

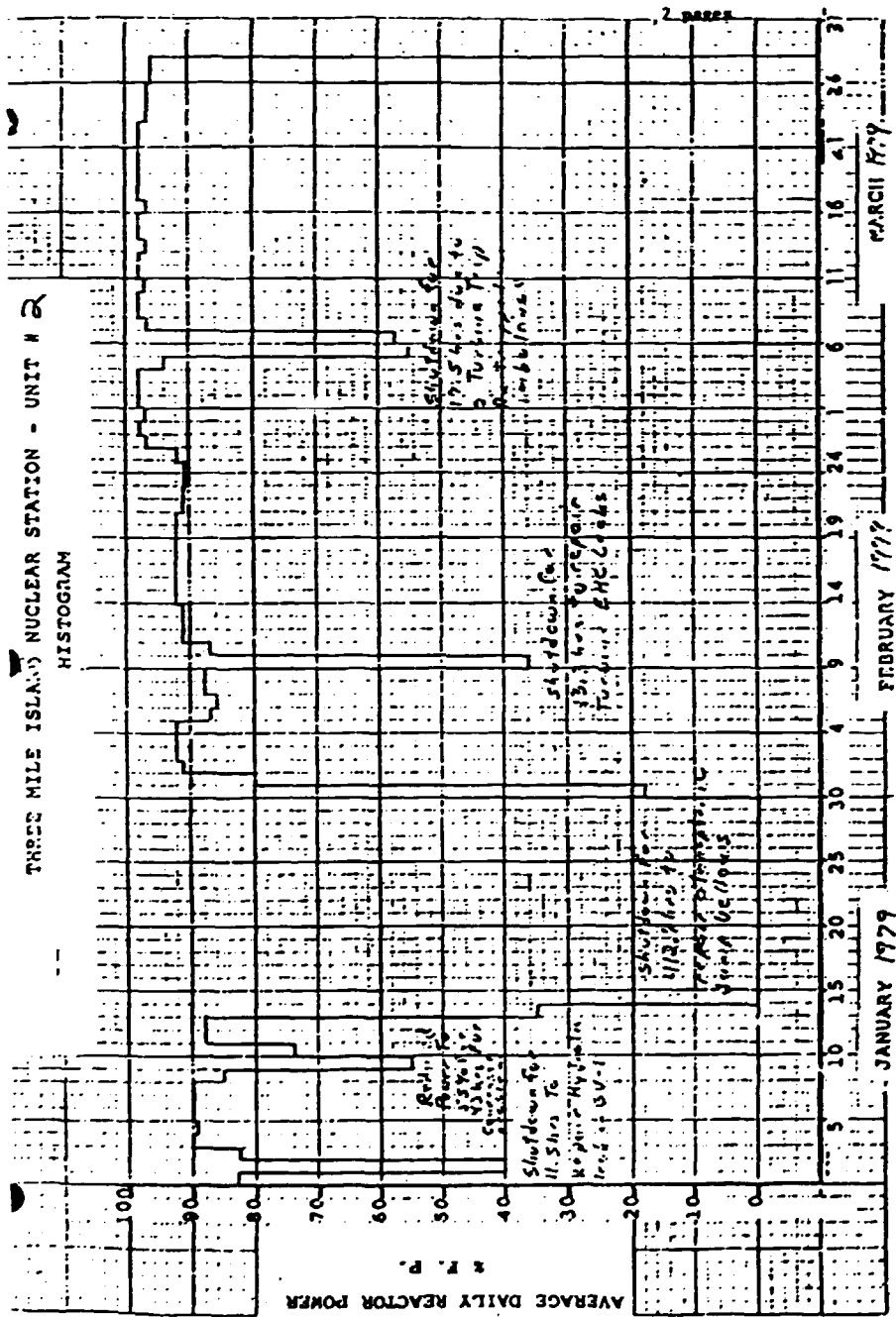


Figure 8 (cont'd). TMI-2 Power History, 1979

Table 12. TMI-2 Soluble Boron History

Reference: TMI Unit 2 Chemistry Log Book 1978, 1979
 Reel No. CHEM-2-002

from Reactor Coolant Letdown Line

Date	Boron (ppm)
3/31/78	1565
4/7	1542
4/14	1158
4/21	1318
5/14	1651
5/21	1668
6/4	1574
8/28	2159
9/10	2090
9/17	1734
9/21	1335
9/28	1254
10/5	1460
10/12	1500
10/17	1158
10/26	1095
11/2	1220
11/9	1595
11/21	1484
12/1	1452
12/9	1071
12/15	1126
12/22	1405
12/29	1109
1/5/79	1088
1/12	1114
1/30	1488
2/6	1075
2/13	1065
2/20	1066
2/27	1058
3/5	1042
3/13	1045
3/20	1035
3/25	1034
3/27	1027

Table 13. k_{∞} of Lattice of Batch "3" Rubble with Burnup (TMI-2)

Case	Burnup Products (Included in Calculation)	k_{∞}^*
1	Depleted ^{235}U , at 2.67 wt %	0.9633
2	Depleted ^{235}U + Sm	0.9531
3	Depleted ^{235}U , Sm & La	0.9530
4	Depleted ^{235}U , Sm, La & Ce	0.9530
5	Depleted ^{235}U , Sm, La, Ce & Eu	0.9527
6	Depleted ^{235}U & 50% of Sm, La, Ce, & Eu	0.9579
7	Pu Isotopes, only (with fresh fuel)	1.0100
8	Depleted ^{235}U , Pu, Sm, La, Ce & Eu	0.9768
9	Depleted ^{235}U , Pu, Sm, La, Ce, Eu, Pm, Nd & Pr	0.9747

$$\% \Delta k_{\infty} = 1.76\%$$

* For fresh fuel assay (2.96) and no fission product, $k_{\infty} = 0.9922$

During the review of this burnup analysis, a concern was raised that it does not account for the axial variation of the exposure history for each fuel assembly. A brief investigation was conducted on the importance of this effect. Each fuel assembly can be considered to have seven axial zones determined by the location of the spacer grids. The Defueling Design Team supplied information on the burnup of each of these zones in the format of Figure 7. An inspection of the information indicated that the lowest burnup was for the top zone (745 to 1501 MWD/MTU), followed by the bottom zone (986 to 2674 MWD/MTU). For the middle five zones the burnup ranges from 1479 to 4567 MWD/MTU. However, for any particular batch "3" assembly, the burnup of any of the middle five zones varies by no more than 15% from the average for those zones. On the basis of these observations, it was decided to treat the batch "3" fuel as three average burnups corresponding to core averages for the top, middle five, and bottom axial zones. Scaling these averages as described in step 1 above resulted in March 28, 1979 values of 1243, 3036 and 1856 MWD/MTU, respectively. Assuming a linear variation of nuclide concentrations with exposure, the uranium, plutonium and fission product number densities were established for these three exposures by adjusting the values previously determined for the batch "3" average exposure.

The 3-zone-sphere model of Case A' in Table 9 was modified with two additional zones for the batch "3" fuel. The central zone contained the minimum exposure, 1243 MWD/MTU, fuel out to a radius of 55.55 cm. This was followed by the 1856 MWD/MTU burnup fuel to an outer radius of 69.99 cm. The remainder of the batch "3" volume (outer radius: 106.26 cm) was filled with the 3036 MWD/MTU burnup fuel. The balance of the model was the same as that described in Table 6. The effective multiplication factor for this system as calculated with XSDRNPM was 0.95598. The corresponding value calculated by KENO V.a was 0.95588 ± 0.00152 . Comparison with the results for Case A' in Table 9 yields a burnup segregation effect of, at most, 0.2% Δk . The small magnitude of this effect coupled with the very low probability of the rubble being segregated by fuel burnup effectively counters the concern about ignoring the axial variation of the burnup for the batch "3" fuel.

III. BENCHMARK CRITICAL EXPERIMENTS

The general performance of the 27 group ENDF/B-IV cross section library for low-enriched, water-moderated systems was included in the earlier discussion on analytical methods. For the purpose of validating the lower-vessel rubble study, a set of 10 critical experiments was selected from an extensive list of candidates compiled by R. L. Murray¹¹ in consultation with staff members of the Babcock & Wilcox Company and Bechtel-Design Engineering. These experiments were chosen to emphasize the relatively hard neutron spectrum resulting from the high soluble boron and low water content of the TMI-2 fuel rubble at optimum moderation.

The 10 critical experiments were selected from the results of three experimental programs. In the B&W "spectral shift"¹² and Argonne "high conversion"¹³ experiments, uniform pin lattices were subjected to soluble-boron-level or lattice-pitch variations to change the neutron spectrum. The B&W "close-packed modules"¹⁴ experiments simulate 25 fuel assemblies at various stages of compaction and driven critical by neutron moderation due to the water gaps between the assemblies. The latter set of experiments also included a soluble boron variation.

Each of the experiments was analyzed with the 27 group ENDF/B-IV cross sections applied in KENO V.a. Four of the experiments (ANL-3, -11, -13, B&W-2452) were modeled with homogeneous fuel regions with cell-averaged constants obtained with XSDRNPM. The results of the analyses are given in Table 14.

The results for the uniform lattice experiments (B&W-10, -11, -12, -13, ANL-3, -11, -13) are consistent with the earlier observations based on the summary of analyses in Table 1. That is, this cross section library yields critical values for well-moderated systems and a negative bias for low-moderated systems. The bias does not appear to be affected by the soluble boron level.

The results for the "close-packed modules" (B&W-2452, -2485, -2500) do not show a consistent trend with either neutron moderation or soluble boron level. The presence of the borated water gaps between the modules could be a factor in the relatively poor analytical performance for these systems.

The results of this limited series of analyses support a 2.5% Δk analytical bias, taking the worst case and statistical uncertainty as a bounding value.

Table 14. Analysis of Critical Experiments for TMI-2 Benchmarking^a

Series	Case	Enrichment (Wt %)	Boron (WPPM)	Moderating Ratio ^b	H ₂ O/Fuel Vol. Ratio	Multiplication Factor	Microfiche Identifier	Microfiche Identifier & Date
B&W	10	4.02	0	2.17	1.14	1.0062±0.0038	PBFBW10	07/05/85
"Spectral Shift"	11	"	1152	2.02	"	0.9961±0.0040	PBFBW11	07/09/84
	12	"	2342	1.88	"	1.0087±0.0032	PBFBW12	07/09/84
	13	"	3389	1.77	"	1.0088±0.0035	PBFBW13A	07/25/84
Argonne	3	3.042	0	3.33	1.37	1.0008±0.0041	PBFHOMO	06/15/84
"High Conversion"	11	"	"	1.90	0.75	1.0008±0.0039	PBFHOMO	06/12/84
	13	"	"	1.13	0.43	0.9861±0.0039	PBFHOMO	06/05/84
B&W	2452	2.549	435	0.50	0.15	0.9961±0.0038	PBFCS27	06/05/84
"Close- Packed Modules"	2485	"	886	1.15	0.38	0.9800±0.0018	PBF248	09/25/84
	2500	"	1156	2.67	1.01	0.9942±0.0019 0.9835±0.0017	PBF2485 PBF2500	09/25/84 09/25/84
TMI-2 "Pin Cell"	Undamaged	2.57	3500	2.98	1.65	0.9492		
	Damaged	"	5000	1.49	0.72	0.9913		

^aSCALE 27 Group ENDF/B-IV Library in KENO-V.a, 2nd Analysis of B&W-2485 was Performed with the
SCALE 123 Group GAM-THERMOS Library.

^bTable 2, R. L. Murray to D. S. Williams, "Selection of Critical Experiments,"
April 5, 1984. This is the ratio of slowing-down power to thermal absorption.

IV. SUMMARY REMARKS

Consistent with the "bounding" approach adopted by the TMI-2 Criticality Task Force, a two-level study has been performed to first, optimize the fuel rubble in terms of maximum reactivity, and second, place the entire core as optimized rubble into the lower vessel in maximum credible (albeit highly improbable) configurations. Having established system multiplication factors for fresh fuel in spherical models at various boron levels, additional analyses conservatively incorporated the consideration of fuel burnup. Finally, in the lenticular model, the curvature of the rubble was allowed to follow that of the vessel wall.

A separate analytical benchmarking study was performed to establish the performance of the analytical data and methods for low-moderated, highly-borated systems. The results of the analysis of ten critical experiments support a 2.5% Δk analytical bias, taking the worst case and statistical uncertainty as a bounding value.

With this analytical bias and an overall shutdown criterion of $k_{\text{eff}} = 0.990$, Case D'" of Table 9 ($k_{\text{eff}} = 0.9646 \pm 0.0017$) becomes the design basis case for limiting boron letdown. That is, a value of 4350 WPPM soluble boron becomes the lower limit for the boron concentration for all accident scenarios involving the dilution of boron in the primary coolant system.

In addition to providing this limiting boron concentration, reactivity effects were determined for a number of parametric variations, including fuel enrichment, shape, volume fraction, temperature, inventory, burnup and system geometry, boron level, reflection and fuel arrangement by zone.

REFERENCES

1. R. M. Westfall, J. T. West, G. E. Whitesides and J. T. Thomas, "Criticality Analyses of Disrupted Core Models of Three Mile Island Unit 2," ORNL/CSD/TM-109 (1979).
2. J. T. Thomas, "Nuclear Criticality Safety Studies of Interest to TMI-2 Recovery Operations," ORNL/CSD/TM-186 (1982).
3. J. R. Worsham, III, F. M. Alcorn, L. A. Hassler, G. M. Jacks, F. G. Welfare, J. J. Woods, "Methods and Procedures of Analysis for TMI-2 Criticality Calculations to Support Recovery Activities Through Head Removal," BAW-1738 (1982).
4. Bechtel Northern Corporation, "Quick Look Inspection: Results Volume II," GEND-030 (1983).
5. J. T. Thomas, "The Effect of Boron and Gadolinium Concentration on the Calculated Neutron Multiplication Factor of $U(3)O_2$ Fuel Pins in Optimum Geometries," ORNL/CSD/TM-218 (1984).
6. C. V. Parks, Editor, "SCALE, A Modular Code System for Performing Standardized Analyses for Licensing Evaluation," Vols. 1, 2, 3, NUREG/CR-0200 (Rev. 3) (1984).
7. R. M. Westfall and J. R. Knight, "SCALE System Cross Section Validation with Shipping-Cask Critical Experiments," Trans. Am. Nucl. Soc., 33, p. 368 (1979).
8. L. M. Petrie and J. T. Thomas, "Assessment of Computational Performance in Nuclear Criticality," ORNL/CSD/TM-224 (1985).
9. H. M. Cundy and A. P. Rollett, Mathematical Models, page 197, Oxford Press (1961).
10. E. W. Barr, J. P. Colletti, J. A. Easly, and J. D. Loma, "TMI-2 Post-Accident Criticality Analysis," GPU-TDR-049 (August 31, 1979).
11. L. Murray to D. S. Williams, "Selection of Critical Experiments," Letter Report (April 5, 1984).
12. T. C. Engelder et al., "Spectral Shift Control Reactor Basic Physics Program, Critical Experiments on Lattices Moderated by D_2O-H_2O Mixtures," BAW-1231 (December 31, 1961).
13. A. R. Boynton et al., "High Conversion Critical Experiments," ANL-7203 (January 1967).
14. G. S. Hoovler et al., "Critical Experiments Supporting Underwater Storage of Tightly Packed Configurations of Fuel Pins, BAW-1645-4 (November 1981).

APPENDIX

Effect of Rubble Particle Size on Lower-Vessel Models

New observations of large chunks of apparently once-molten and resolidified UO_2 present in the TMI-2 lower vessel have brought into question the assumption on UO_2 particle size that was adopted by the Criticality Task Force in 1984. In the previous lower-vessel analyses, it was assumed that the most reactive fuel particle size was that of the design fuel pellet. A study has been undertaken to determine if a larger, reconfigured pellet might be more reactive.

The design pellet size corresponds to a spherical particle of 1.0724 cm in diameter. An extensive series of lattice cell calculations was performed to determine the optimum fuel volume fraction for a variety of particle sizes larger than the design pellet. Several observations can be drawn from the results of this study, which is summarized in Table A1.

1. The most reactive fuel particle has a diameter between 2.2 and 4.4 cm and a volume fraction between 0.65 and 0.67 (for a boron level of 4350 WPPM).
2. The same behavior is seen for both the batch "3" (2.96% enrichment) and "1" and "2" average (2.34% enrichment) with a relatively constant reactivity difference of between 6 and 6.7% Δk .
3. For the largest particle studied, the maximum multiplication factor occurred for the volume fraction corresponding to the theoretical maximum packing fraction.

On the basis of these observations, an overall optimum particle diameter of 3.5 cm at a fuel volume fraction of 0.66 was chosen for application in the finite system analyses. A single cell calculation with these specifications confirmed the projected maximum multiplication factor.

The finite system models were defined to demonstrate the reactivity effects of various modifications to the defueling design basis case (Model D" in Table 9). The major features of these modifications are based on current core damage assessments which include an estimated 20 to 30% core melt with a high likelihood of the molten fuel being from batches "1" and "2". The approach taken in modifying the design basis case was to introduce the optimum-particle-size fuel into the central, most-reactive zone of the models.

Five new models were analyzed. The results of these analyses are summarized in Table A2. The infinite lattice multiplication factors for the new materials, as well as for the materials already present in the design basis case, are summarized in Table B3. In treating the burnup for batches "1" and "2", a conservative procedure was applied in adopting information from the previous burnup analysis of the batch "3" fuel. The negative reactivity components, i.e., ^{235}U depletion and fission product generation, were determined on the basis of the lower batch "3" burnup. However, the positive reactivity component due to plutonium generation was determined on the basis of the higher burnups for batches "1" and "2".

Returning to Table A2, several observations can be drawn from the analysis of the finite systems.

1. Comparison of Cases D'' and I' shows a small positive effect due to the assumption that 20% of the core average fuel has the optimum particle size. However, this difference is not statistically meaningful. Comparison of the discrete ordinates results (Cases D''' and I) shows no difference.
2. Progressively adding burnup and going from 20% to 30% of the inventory (Cases I, J, K) shows a sequential decrease in the multiplication factor.
3. The Smith-Hopkins model incorporates the likelihood that all of the molten fuel was from batches "1" and "2". The Murray model has the batch "3" fuel on the periphery of the system, corresponding to its location in the reactor core. Both of these features substantially reduce the multiplication factor below the design basis value.

The overall conclusion of this study is that while a larger particle size was determined to be more reactive than the design pellet, incorporation of the larger particle into finite systems that are consistent with the core damage assessment leads to a reduction in the system multiplication factor.

Table A1. Summary of Particle Size Study¹

Sphere Dia. (cm)	Optimum Fuel Volume Fraction	$U(2.96)O_2k_\infty^4$	$U(2.34)O_2k_\infty^5$
1.072 ²	0.61	1.0064	0.9382
1.4	0.61	1.0132	0.9462
1.6	0.62	1.0168	0.9494
2.2	0.65	1.0234	0.9571
3.5	0.66	1.0265	
4.4	0.67	1.0246	0.9611
6.6	0.69	1.0144	0.9513
8.8	0.74 ³	1.0024	0.9427

¹Spherical Cell Model, Boron at 4350 WPPM²Corresponds to Design Pellet³Spheres Touching, Maximum Packing Fraction⁴Maximum Values Calculated, Single Value at 3.5 cm⁵Maxima 0.05 to 0.1% Δk Larger at VF+0.01

Table A2. Finite Systems with Optimum Fuel Particle Size

Case	Inventory	Geometry	Multiplication Factor	Microfiche (data)
D ^{**} (Design Basis)	60 Assy "3," Burned 117 Assy "1" & "2"	3 Zone Lenticular	0.9646±0.0017	JRKTMIIG 10/06/84
D ^{**} (Spherical Eq.)	60 Assy "3," Burned 117 Assy "1" & "2"	3 Zone Sphere	0.9671	
I [†] (Bradbury 20)	35.4 Assy "1", "2", "3", Opt. 48 Assy "3" Burned 93.6 Assy "1" & "2"	4 Zone Sphere	0.9690	JRKTMIIL 04/29/85
I [†] (Bradbury 20)	35.4 Assy "1", "2", "3", Opt. 48 Assy "3" Burned 93.6 Assy "1" & "2"	4 Zone Lenticular	0.9663±0.0019	JRKTMIIL 04/30/85
J [†] (Bradbury 20B)	35.4 Assy "1", "2", "3", Opt. Burned 48 Assy "3" Burned 93.6 Assy "1" & "2"	4 Zone Sphere	0.9624	JRKTMIIL 05/02/85
J [†] (Bradbury 20B)	35.4 Assy "1", "2", "3", Opt. Burned 48 Assy "3" Burned 93.6 Assy "1" & "2"	4 Zone Lenticular	0.9618±0.0018	JRKTMIIL 05/03/85
K [†] (Bradbury 30B)	53.1 Assy "1", "2", "3", Opt. Burned 42 Assy "3" Burned 81.9 Assy "1" & "2"	4 Zone Sphere	0.9618	JRKTMIIG 05/02/85
L [†] (Smith-Hopkins 20)	23.4 Assy "1" & "2" Opt. Burned 60 Assy "3" Burned 93.6 Assy "1" & "2"	4 Zone Sphere	0.9576	JRKTMIIL 05/02/85
M [†] (Murray 20)	23.4 Assy "1" & "2" Opt. Burned 93.6 Assy "1" & "2" 60 Assy "3" Burned	4 Zone Sphere	0.9385	JRKTMIIL 05/02/85

[†]All systems have boron levels of 4350 WPPM and an 8-in.-thick SS-304 reflector.

[‡]Optimum particle size in central zones, 3.5-cm diameter, fuel volume fraction = 0.66.

Table A3. Infinite Lattice Cell¹ Analyses for Cross-Section Generation

Fuel Type	Fuel Enrichment ² (wt % ^{235}U)	Fuel Volume Fraction	Multiplication Factor
"3" Burned	2.67	0.61	0.9881
"1" & "2"	2.34	0.61	0.9382
"1", "2", "3" Opt.	2.57	0.66	0.9882
"1", "2", "3" Opt. Burned	2.32	0.66	0.9784
"1" & "2" Opt. Burned	2.11	0.66	0.9594

¹Spherical particles in dodecahedral cell, boron at 4350 WPPM.

²Burned compositions contain fission products and plutonium.

ORNL/CSD/TM-222

INTERNAL DISTRIBUTION

1. J. E. Bigelow	27. A. M. Perry, Jr.
2. J. A. Bucholz	28. L. M. Petrie
3. R. P. Leinius/G. E. Whitesides	29. T. H. Row
C&TD Library	30. J. S. Tang
4. E. D. Collins	31. J. T. Thomas
5. W. K. Crowley	32-36. J. C. Turner
6. H. R. Dyer	37. M. W. Waddell
7-11. P. E. Fox	38-42. R. M. Westfall
12. R. Gwin	43-44. Central Research Library
13-17. O. W. Hermann	45. Y-12 Document Reference Section
18. C. M. Hopper	46-47. Laboratory Records
19. W. C. Jordan	48. Laboratory Records - RC
20-24. J. R. Knight	49. ORNL Patent Section
25. N. F. Landers	50. K-25 Plant Library
26. C. V. Parks	

EXTERNAL DISTRIBUTION

51. B. J. Snyder, U. S. Nuclear Regulatory Commission, Washington, DC 20555
52. Division of Engineering, Mathematics and Geosciences, U. S. Department of Energy, Washington, DC 20545
53. F. Alcorn, Babcock & Wilcox Co., Nuclear Development Center, P. O. Box 1260, Lynchburg, VA 24505
54. T. R. Stevens, Babcock & Wilcox Co., Nuclear Development Center, P. O. Box 1260, Lynchburg, VA 24505
55. G. R. Jacks, Babcock & Wilcox Co., Nuclear Development Center, P. O. Box 1260, Lynchburg, VA 24505
56. J. R. Worsham, Babcock & Wilcox Co., Nuclear Development Center, P. O. Box 1260, Lynchburg, VA 24505
57. W. G. Pettus, Babcock & Wilcox Co., Nuclear Development Center, P. O. Box 1260, Lynchburg, VA 24505
58. L. A. Hassler, Babcock & Wilcox Co., Nuclear Development Center, P. O. Box 1260, Lynchburg, VA 24505
59. P. C. Childress, Babcock & Wilcox Co., Nuclear Development Center, P. O. Box 1260, Lynchburg, VA 24505
60. W. E. Austin, GPU Nuclear Corporation, P. O. Box 480, Middletown, PA 12057-0191
61. W. Bixby, U. S. Department of Energy, P. O. Box 88, Middletown, PA 17057
62. P. Bradbury, Bechtel, Inc., P. O. Box 72, Middletown, PA 17057
63. T. Brown, Los Alamos National Laboratory, P. O. Box 1663, Los Alamos, NM 87544
64. K. M. Burton, EG&G Idaho, Inc., P. O. Box 88, Middletown, PA 17057
65. R. L. Egli, Dep. Asst. Manager for Energy Research and Development, U. S. Department of Energy, Oak Ridge Operations, Oak Ridge, TN 37830

66. W. A. Franz, EG&G Idaho, Inc., P. O. Box 88, Middletown, PA 17057
67. R. F. Hansen, GPU Nuclear Corporation, P. O. Box 480, Middletown, PA 17057
68. I. E. Fergus, GPU Nuclear Corporation, P. O. Box 480, Middletown, PA 17057
69. G. R. Skillman, GPU Nuclear Corporation, P. O. Box 480, Middletown, PA 17057
70. R. A. Knief, GPU Nuclear Corporation, P. O. Box 480, Middletown, PA 17057
71. W. C. Hopkins, Bechtel, Inc., 15740 Shady Grove Road, Gaithersburg, MD 20877-1454
72. P. S. Kepley, Bechtel, Inc., 15740 Shady Grove Road, Gaithersburg, MD 20877-1454
73. D. J. McGoff, U. S. Department of Energy, Washington, DC 20545
74. T. McLaughlin, Los Alamos National Laboratory, P. O. Box 1663, Los Alamos, NM 87544
75. R. L. Murray, P. O. Box 5596, Raleigh, NC 27650
76. R. L. Rider, Bechtel, Inc., 15740 Shady Grove Road, Gaithersburg, MD 20877-1454
77. C. L. Ried, Bechtel, Inc., 15740 Shady Grove Road, Gaithersburg, MD 20877-1454
78. J. N. Rogers, Div. 8324, Sandia Laboratories, Livermore, CA 94550
79. D. R. Smith, Los Alamos National Laboratory, P. O. Box 1663, MS-560, Los Alamos, NM 87544
80. W. R. Stratton, Los Alamos National Laboratory, P. O. Box 1663, Los Alamos, NM 87544
81. E. Walker, Bechtel, Inc., P. O. Box 3965, San Francisco, CA 94119
82. R. Smith, Bechtel, Inc., P. O. Box 3965, San Francisco, CA 94119
83. D. S. Williams, Bechtel, Inc., 15740 Shady Grove Road, Gaithersburg, MD 20877-1454
84. M. N. Baldwin, Babcock & Wilcox Co., Nuclear Development Center, P. O. Box 1260, Lynchburg, VA 24505
- 85-111. Technical Information Center, U. S. Department of Energy, Oak Ridge, TN 37830